

AIRBORNE SOUND BASED DAMAGE DETECTION FOR WIND TURBINE ROTOR BLADES USING IMPULSE DETECTION IN FREQUENCY BANDS

THOMAS KRAUSE, STEPHAN PREIHS, JÖRN OSTERMANN

Institut für Informationsverarbeitung
Leibniz Universität Hannover
Appelstraße 9a, 30167 Hannover, Germany
e-mail: {krause, preihs, ostermann}@tnt.uni-hannover.de

Keywords: Acoustic emission, damage detection, wind turbine rotor blade, airborne sound

Summary: This paper presents a cracking sound detection algorithm for damage detection of wind turbine rotor blades.

1 ABSTRACT

Composite rotor blades of wind turbines are subjected to high static and dynamic loads. The load can cause small damages which can accumulate over time to critical structural damage. A system detecting defects in early stages helps to react fast and avoid critical damage. Such a method will enable the wind turbine operator to increase safety and minimize the economical burdens caused by downtime, repairing, replacing and maintenance. Therefore many research projects try to pave the way to a reliable and practical early damage detection system for wind turbine rotor blades.

One promising approach is acoustic emission event detection. Acoustic emission stands for stress waves emitted by a damage process. While other acoustic emission approaches use ultrasonic surface acceleration as input signals, we propose using the airborne sound in audible frequencies. The aim is to detect cracking sounds emitted by the damage process. In this paper we present an improved version of our algorithm for detecting these cracking sounds by using impulse detection in individual frequency bands. The performance with the new algorithm increased significantly. In the recordings of a 76 day full scale rotor blade fatigue test we detected 104 cracking sounds while there were only six false positive detections. Compared with the previous algorithm, the amount of detected cracking sounds is about three times higher and there are significantly less false alarms.

2 INTRODUCTION

Wind turbine rotor blades have to match the criteria of being light weight and large at the same time. Therefore all modern blades are made of composite materials. During operation the blades are subjected to high static and dynamic loads. This permanent load can lead to small damages which accumulate over time to critical structural damage. In situations where damage occurs in an important part of a structure, structural health monitoring systems can be able to improve safety and minimize the costs for maintenance, repairing and replacing. Therefore the damage has to be detected in early stages to react fast and avoid critical damage. In modern wind turbines controlling units are already implemented like the blade pitch control or an emergency shut-off system. These systems might be also triggered by a structural health monitoring system to avoid critical damage.

There are two certified rotor blade monitoring systems on the market [1] which are able to detect ice, but these systems are not capable of detecting damage in early stages. Many

research results of nondestructive testing methods were published so far. Several approaches can be used for automatic damage detection of wind turbine rotor blades. An overview can be found in [2] [3]. For detecting damage automatically, reliably and in early stages many research projects focus on the acoustic emission event detection approach. The aim of this approach is to detect components of the stress wave caused by the damage process. For this sensors mounted on the surface of the blade are used. With this approach small damages can be detected [2] [3] [4] [5]. The sensors operate in ultrasonic frequencies, therefore the amount of sensors is relatively high due to the size of modern blades and high internal damping of composite materials [4] [5].

Using acoustic emission for damage detection in an operating wind turbine is an unsolved problem. The higher risk of damage from lightning strikes caused by the electrical conductive wires is the main problem which prevents testing an acoustic emission approach in an operating rotor blade. So far there are only few results published using an acoustic emission system in an operating wind turbine rotor blade. The ability of detecting damage while operation could not directly been tested due to the lack of damage. Environmental noise during operation was observed which has to be taken into account to avoid false detections [6] [7].

In contrast to existing approaches, in [9] we proposed a damage detection approach by identifying cracking sounds in audible frequencies from 20 Hz to 20 kHz using the airborne sound. The idea is based on the observation of audible cracking sounds during rotor blade tests [8]. We assume that only up to three sensors are necessary for monitoring the whole rotor blade due to the relatively low attenuation of the air in such frequencies. In addition, fiber optic microphones can be used for recording sound inside a rotor blade. Their cords are optical fibers which are non-metal, so they do not increase the risk of damage from lightning strikes. This makes the approach applicable in an operating rotor blade.

3 CRACKING SOUND MODEL

In [9] we presented the first results of using airborne sound for rotor blade damage detection. In that paper a model of impulse-like cracking sounds is described. The model was developed using airborne sound recordings during parts of a certification test of a 55 m rotor blade. The recordings consisted of one 76 day flapwise fatigue test and four static tests which took about ten minutes each. The sound was recorded inside the rotor blade using three electrical microphones and one fiber optic microphone.

With this recordings a model of the cracking sound was developed. The model is further described by an example cracking sound in the static test recordings with low environmental noise. A part of the recording is displayed using the power spectrogram (Figure 1). The cracking sound is displayed in the spectrogram as triangular shaped area. The power in very low frequencies is noise from the rotor blade test.

The first characteristic of the cracking sound model is the impulse-like increase in power which can be found at 0.15 s in Figure 1. The maximal power occurs in this time period which we refer to as first part of the impulse. Subsequently there is an approximately exponential decrease in power over time. In Figure 1 the power is displayed in decibels, therefore the decrease is approximately linear. The power of every impulse is distributed over a wide frequency range, so the impulses are non-tonal. Depending on the impulse, the frequency where maximum power occurs can vary in a wide range. In our recordings the value occurs in

the range of 150 Hz to 10 kHz. The example impulse has its maximal power at 500 Hz. Another characteristic of all cracking sounds is a specific decrease in power towards higher frequencies, beginning with the frequency where maximal power occurs. The decrease is linear in decibel with a specific constant slope.

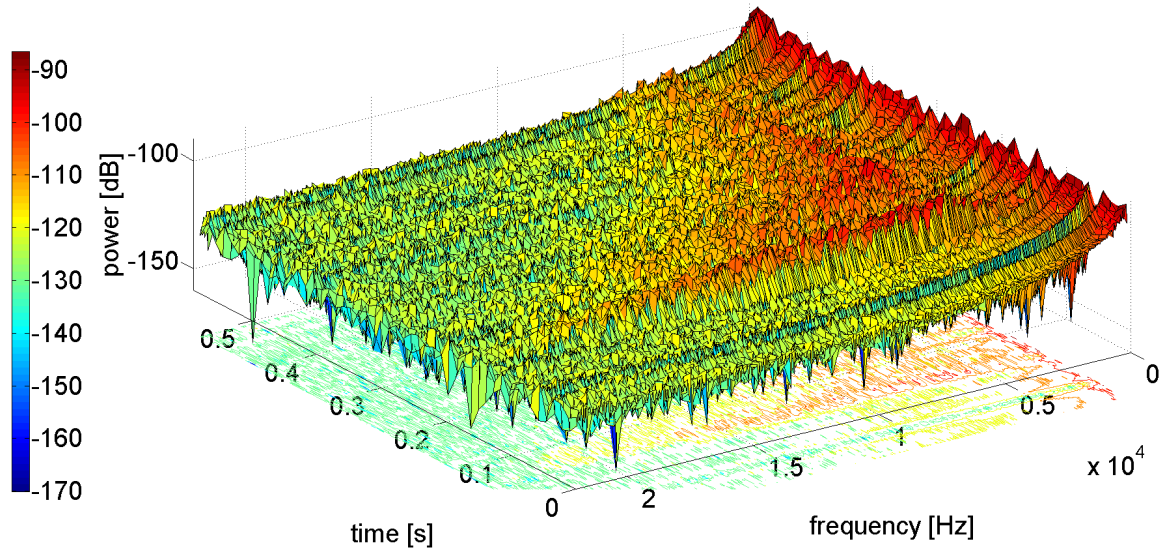


Figure 1: Power spectrogram with cracking sound and minor noise of the rotor blade test.

4 DETECTION ALGORITHM

In [9] we also presented a cracking sound detection algorithm which is based on the comparison of the input signal with the cracking sound model. In this paper an improved detection algorithm is presented, including an impulse detection feature based on individual frequency bands and a procedure for the extraction of frequency boundaries.

The detection algorithm uses five audio features $f_1 - f_5$ to represent the model characteristics. The features are based on the power spectrum $P(k,l)$ calculated by a windowed short time fourier transform. Here k is the frequency index and l the time index. All features are compared with threshold parameters δ to see if the signal is similar to the cracking sound model. The principle flow chart of the algorithm is displayed in Figure 2. The power gradient feature and the bandwidth at which the signal is impulse-like are responsible for the improved performance of the current algorithm. In the following Subsections all important steps of the detection algorithm are described.

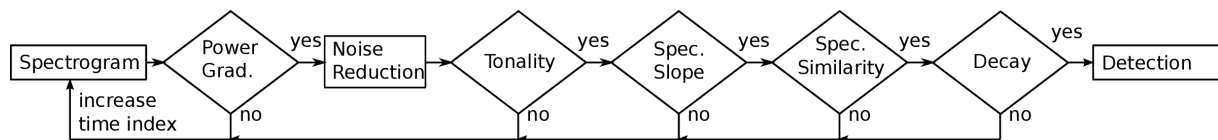


Figure 2: Flow chart of the detection algorithm.

a. Power gradient feature

In the previous algorithm, the first feature was the increase in power over all frequencies which displayed if the signal is impulse-like. This led to missed impulse-like sounds when at the same time an impulse and a noise signal with high decrease in power occurred. So we modified this feature. The power gradient feature used now analyzes if the signal is impulse-like over a wide frequency range. For this, the increase in power in all frequency bands is calculated by Equation 1. The raising time of the impulse model is denoted by l_i . If the increase in power is greater than the threshold g_b , the frequency band is defined as impulse-like. The power gradient feature f_1 is the number of all impulse-like frequency bands as shown in Equation 2. Very low frequencies are left out. These frequencies can provide high power and are not correlated with the cracking sound. The frequency range reduction is adjusted with the parameter k_s .

$$g(k, l) = \begin{cases} 1, & \text{if } P(k, l) - P(k, l - l_i) > g_b \\ 0, & \text{else} \end{cases} \quad (1)$$

$$f_1(l) = \sum_{k=k_s}^{k_{end}} g(k, l) \quad (2)$$

If a significant number of bands shows a sudden power increase the feature exceeds the threshold parameter $\delta_{1, \min}$ and the signal becomes a candidate for a cracking sound with the time index l_c and is further processed.

The frequency bands where the signal is impulse-like is extracted and used for the features processed after the power gradient feature. Frequency components which are out of the impulse-like frequency bandwidth are not taken into account. This leads to a better separation of noise when checking the three features tonality, spectral slope and spectral similarity. The bandwidth is approximated by combining all bands where the power increases, if the frequency gap between the bands is smaller than a defined boundary. If the amount of combined impulse-like frequency bands is greater than one, the band k_w with the widest bandwidth is taken. The boundary frequencies indices k_b and k_e are used for further processing.

$$k_b \leq k_w \leq k_e \quad (3)$$

b. Noise reduction

In case a power gradient according to the model is observed, the algorithm reduces the influence of not impulse-like signals in the power spectrogram by using spectral subtraction. The assumption for spectral subtraction is a stationary signal. This assumption is approximately valid if a short time period is taken. The signal model specifies that the rise time of the power is shorter than the decay time. Therefore the subtracting spectrum is taken a short time period before the beginning of the impulse, at the time $l_c - l_r$. The noise reduced spectrogram P_s is only used for calculating features taken from the first part of the impulse.

$$P_s(k, l_c) = 10 \log_{10} [P(k, l_c) - P(k, l_c - l_r)] \quad (4)$$

c. Tonality feature

There are three features calculated using the noise reduced power spectrum of the first part of the impulse. The first feature represents the tonality of the signal. For this the spectral flatness measure [10] is used. The geometric mean of the power spectrum is divided by the arithmetic mean as shown in Equation 5.

$$f_2(l_c) = \frac{\left(\prod_{k=k_b}^{k_e} P_s(k, l_c) \right)^{\frac{1}{k_e - k_b}}}{\frac{\sum_{k=k_b}^{k_e} P_s(k, l_c)}{k_e - k_b}} \quad (5)$$

The result is a value between zero and one. Where zero represents a maximal tonal signal and one a maximal noise-like signal. The cracking sound model specifies the sound as non-tonal so the feature value should not be lower than the threshold $\delta_{2,\min}$.

d. Spectral slope feature

The second feature, using the noise reduced power spectrum of the first part of the impulse, is the specific slope in the power spectrum. This feature represents the linear decrease in decibel towards higher frequencies, beginning at the frequency k_p where maximal power occurs. This frequency has to be taken from the interval k_w . The gradient f_3 of a simple linear regression is calculated as an approximation of the signal slope by

$$f_3(l_c) = \frac{\sum_{k=k_p}^{k_e} (k - \bar{k})(P_s(k, l_c) - \overline{P_s(l_c)})}{\sum_{k=k_p}^{k_e} (k - \bar{k})^2} \quad (6)$$

The overbar in Equation 6 means the arithmetic mean using the frequency interval k_p to k_e . The upper and lower threshold parameter $\delta_{3,\max}$ and $\delta_{3,\min}$ define the allowable deviation from the characteristic model slope. In Figure 3 the power spectrum of the first part of the cracking sound is displayed. The frequencies f_p and f_e are corresponding to the frequency indices k_p and k_e .

e. Spectral similarity feature

The third feature, calculated using the noise reduced power spectrum of the first part of the impulse, compares the impulse with the model curve. This feature represents the specific linear decrease in decibel from the frequency with maximal power k_p towards higher frequencies as well as the noise-like characteristic of the impulse.

The power spectrum of the impulse model curve P_{prot} is defined by a characteristic exponential decline of power towards higher frequencies. The representation of the signal in decibel linearises this decline.

The feature f_4 measures the similarity of the signal spectrum and the model spectrum. The similarity is displayed in the euclidean distance normalized by the bandwidth of the spectrum by

$$f_4(l_c) = \frac{1}{k_e - k_p} \sqrt{\sum_{k=k_p}^{k_e} [P_{prot}(k) - P_s(k, l_c)]^2}. \quad (7)$$

The threshold parameter $\delta_{4,max}$ is the upper limit for a positive detection.

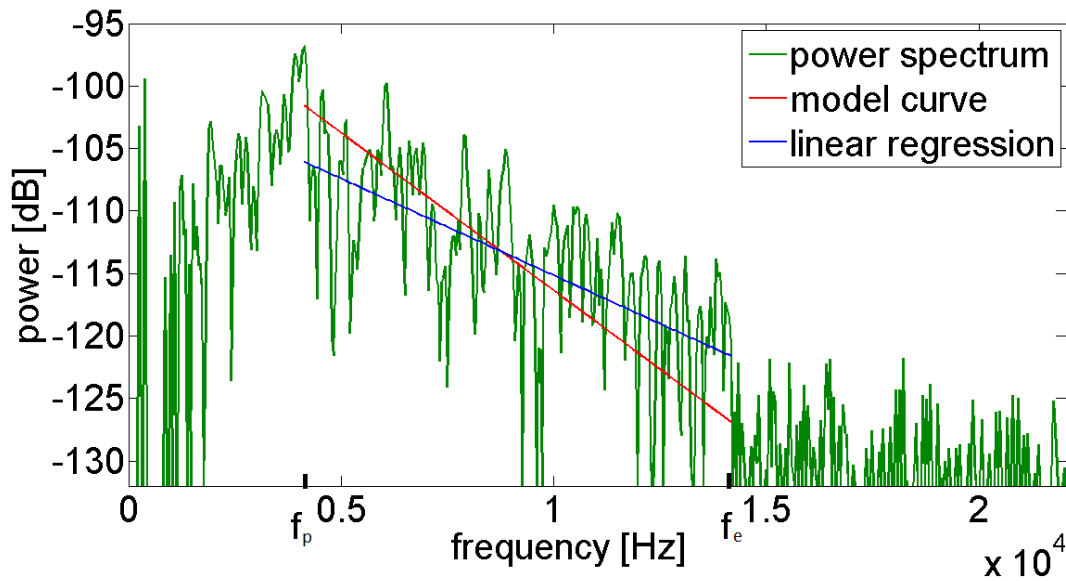


Figure 3: Spectrum of the first part of the impulse, linear regression curve and model curve.

f. Impulse decay feature

The last feature f_5 of the algorithm is the decay of the impulse. The model decay defines a linear decrease in signal power in decibel over time. The feature is calculated using the power over time in the frequency k_p . The time period starts at the time index l_c . The length of the time period is adjusted with the value l_d . The decay of the signal is approximated calculating the gradient of the simple linear regression by

$$f_5(l_c) = \frac{\sum_{l=l_c}^{l_c+l_d} (l - \bar{l}) \left[10 \log_{10}(P(k_p, l)) - 10 \log_{10}(\overline{P(k_p)}) \right]}{\sum_{l=l_c}^{l_c+l_d} (l - \bar{l})^2}. \quad (8)$$

Here the overbar symbolizes the arithmetic mean in the interval of l_c to l_c+l_d . The decay of the example cracking sound and the approximated decay is shown in Figure 4. The time t_c corresponding to the time index l_c and t_d corresponding to l_d are marked in the figure. The upper and lower threshold parameters $\delta_{5,max}$ and $\delta_{5,min}$ define the detection interval for this feature. In case the five features are detected at a time frame l_c the algorithm indicates that a cracking sound has occurred.

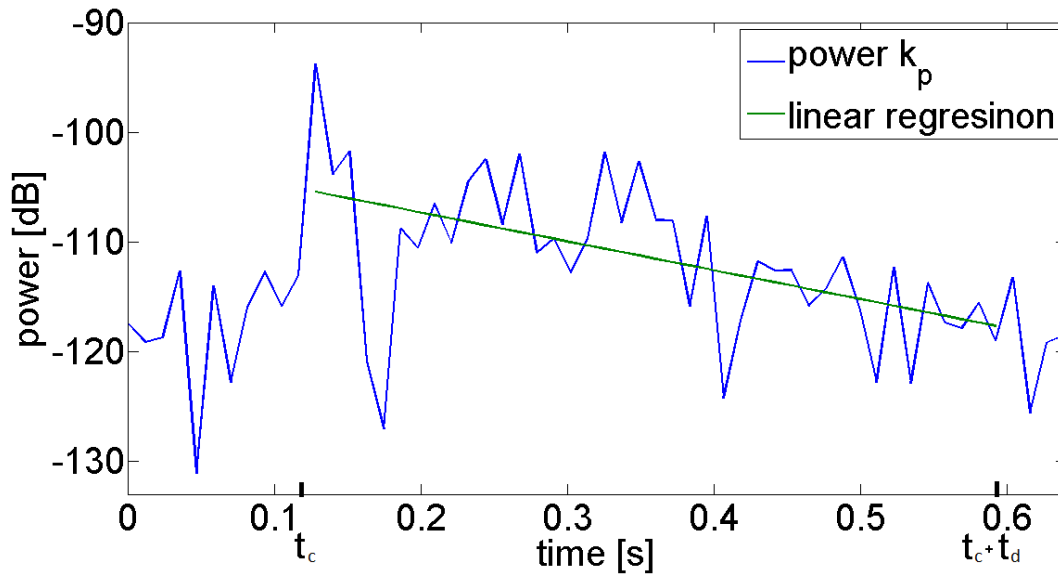


Figure 4: Power over time in frequency with maximal power and linear regression curve.

5 RESULTS

The improved detection algorithm presented in Section 4 was used to process the rotor blade stress test recordings described in Section 3. The data of the recordings was manually labeled. The amount of cracking sounds in the flapwise fatigue test is unknown due to the long recording time. We built a training-set and a test-set by splitting all static test recordings equally and taking one hour of representative fatigue test data for both sets. We assume that the lower power impulses are less important for the damage detection purpose, so we split up the impulse signals into two groups, signals with a signal peak to average noise ratio of less than 30dB were labeled as low power impulses and signals with a ratio of more than 30dB were marked as high power impulses. The recordings of the optical microphone were used to get the further described results. The test-set and training-set are identical to the sets used in the previous publication [9].

With the improved detection algorithm there are only slightly better detection results in the test-set. A sensitivity¹ of 84 % for signals with high power and a sensitivity of 52 % for cracking sounds with low power are achieved while there are no false positive detections. Nevertheless there is a significantly better detection performance in the fatigue test recording. Processing the 76 days fatigue test data provides 104 correctly detected cracking sounds and only six false positive detections. The amount of correctly detected cracking sounds is three times higher compared to the results of the previous algorithm and at the same time the amount of false positive detection decrease from 67 to six. We assume that the higher noise in the fatigue test leads to the better results in this recordings.

No critical structural damage occurred during the rotor blade tests, so in the fatigue test the cracking sounds happened significantly more often in the beginning of the test, where the structure adapted to the load.

¹The sensitivity is the number of correctly identified impulses divides by all impulses in the set.

6 SUMMARY

In this paper, an improved version of an algorithm for detection of impulse-like cracking sounds in rotor blades of wind turbines is presented. The proposed algorithm for damage detection is based on a model of the cracking sound. The model characteristics were displayed in the following features: power gradient, tonality, spectral slope, spectral similarity and decay. All features are calculated and checked by the algorithm. The impulse detection displayed in the power gradient feature was modified to measure the increase in power of frequency bands. With this modification the method is able to separate the decay of tonal background signals and cracking sound impulses. This provides better detection results in the 76 day recordings of full-scale fatigue test, 104 cracking sounds were detected while there are only six false positive detections. Compared with the previous version of the algorithm the amount of detected cracking sounds is about three times higher and the number of false alarms are significantly lower.

7 REFERENCES

- [1] DNV GL SE. List of Certifications - Condition Monitoring Systems (CMS) / Monitoring Bodies for CMS. http://www.gl-group.com/pdf/Condition_Monitoring_System_GL_RC.pdf, July 2014.
- [2] C. C. Ciang, J.-R. Lee, and H.-J. Bang. Structural health monitoring for a wind turbine system: a review of damage detection methods. *Measurement Science and Technology* 19, page 20 ff, 2008.
- [3] P.J. Schubel, R.J. Crossley, E.K.G. Boateng, and et al. Review of structural health and cure monitoring techniques for large wind turbine blades. *RenewableEnergy*, 51:113-123, 2012.
- [4] G. R. Kirikeraa, V. Shindea, M. J. Schulza, and et al. Damage localisation in composite and metallic structures using a structural neural system and simulated acoustic emissions. *Mechanical Systems and Signal Processing*, 21:280–297, 2007.
- [5] A.G. Beattie. Acoustic Emission Monitoring of a Wind Turbine Blade During a Fatigue Test. In 35th Aerospace Sciences Meeting, 1997.
- [6] O. Ley and V.F. Godinez-Azcuaga. A wireless system for structural health monitoring of wind turbine blades. *Safety, Reliability, Risk and Life-Cycle Performance of Structures and Infrastructures*, pages 275–279, 2013.
- [7] M.J. Blanch and A.G. Dutton. Acoustic Emission Monitoring of Field Tests of an operating Wind Turbine. *Key Engineering Materials Vols. 245-246*, pages 475–482, 2003.
- [8] P. A. Joosse, M. J. Blanch, A. G. Dutton, and et al. Acoustic Emission Monitoring of Small Wind Turbine Blades. *Journal of solar energy engineering*, 124(4):446–454, 2002.
- [9] T. Krause, S.Preihs and J. Ostermann. Detection of Impulse-Like Airborne Sound for Damage Identification in Wind Turbine Rotor Blades, EWSHM, 2014.
- [10] A.H. Gray and J.D. Markel. A spectral-flatness measure for studying the autocorrelation method of linear prediction of speech analysis. *IEEE Trans. Acoust. Speech Signal Process.*, 22:207–217, 1974.